ASEAN Engineering Journal

Full Paper

INVESTIGATION OF PSK/QAM MODULATED HYBRID FIBER OPTIC AND FREE SPACE OPTIC SYSTEM UNDER VARIOUS ATMOSPHERIC LOSSES

M Vinoth Kumar[a], Vinod Kumar[b]*, Rupali Singh[a]

[a]Department of Electronics and Communication Engineering, Faculty of Engineering and Technology, SRM Institute of Science and Technology, Delhi-NCR Campus, Modinagar, Uttar Pradesh, India.
[b]Department of Electronics and Communication Engineering,Chandigarh Engineering College, Greater Mohali,Punjab, India.

Article history
Received
06 December 2021
Received in revised form
22 May 2022
Accepted
22 June 2022
Published online
28 February 2023

*Corresponding author
director.academic@cgc.ac.in

Graphical abstract

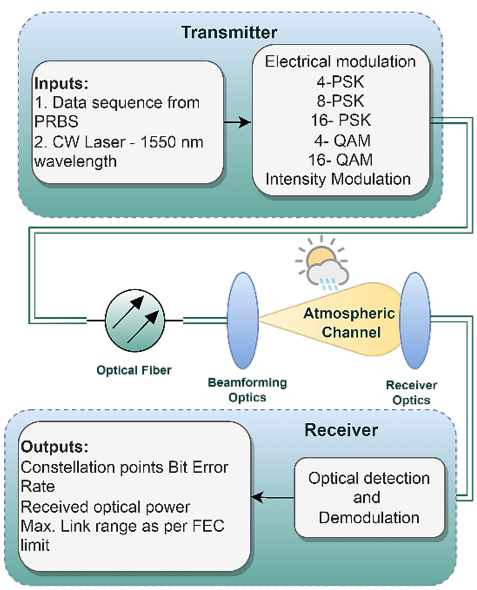

Abstract

This research aims to investigate how effectively digital modulation performs to transfer data via hybrid fiber optic and free space optic (FO-FSO) channels for last-mile communication systems. Digital modulation techniques investigated are phase-shift keying (PSK) 8-PSK, 16-PSK, quadrature amplitude modulation (QAM) 4-QAM, 16-QAM, and 64-QAM. FSO is line-of-sight technology being a solution to a last-mile communication system for the challenge of fiber optic cables installation. Combining FSO with fiber optic technology avoids bending losses and the implementation challenges of fiber optic cables in metropolitan areas and between buildings. But atmospheric challenges such as haze, fog, and rain cause signal loss while transmitting data in free space. Also, atmospheric turbulence and antenna misalignments lead to signal error. This paper proposed the models of QAM and PSK digital modulated signal transmission over FO-FSO and compared the results to better fiber optic-FSO links to achieve a last-mile communication network. This fiber optic and FSO model is analyzed for the distance up to 100 km of fiber optic channel and 0.4-1.5 km of FSO channel. Constellation diagrams and error-vector magnitude (EVM) concerning received power at the receiver are compared to analyze FSO channel capacity for various weather attenuations.

Keywords: Fiber Optics, Free Space Optics (FSO), QAM, PSK, Gamma-Gamma turbulence model

1.0 INTRODUCTION

Due to the increasing demand for bandwidth and high-speed internet connectivity by internet users, researchers have proposed and analyzed several advancements in communication systems, especially for the deployment of 5G networks. In terms of bandwidth, the fiber optic channel is the most efficient communication medium, but it is also the most expensive due to its high implementation and maintenance costs. FSO is becoming the preferred medium for transmission system design engineers in challenging locations such as mountains, metropolitan cities, and buildings where fiber-optic links cannot be efficiently built and high data rate speeds are required [1]. A free space optic (FSO) system does not require any spectrum licensing and does not interfere with radio frequency (RF) bands; FSO has been an exciting research field in optical communication systems. In addition, because of its high-speed, secure point-to-point link and low-cost internet service, FSO has become an alternate channel medium to fiber optic link [2, 3]. The hybrid fiber-wireless optical network is emerging as a primary access network design capable of providing both wired and wireless connectivity to fulfill the large bandwidth, high data rate, and flexible access needed for future generation access networks [1]. Several new concepts for hybrid fiber-wireless access and free space optical channel have recently been reported [4-7]. Millimeter/Radio over fiber with independent wired and wireless signals have been studied with various modulators [4, 8]. A full-duplex hybrid fiber-wireless link with QAM signals link was modeled and analyzed to implement in the future wired and integrated wireless network [9]. Models given in [10] show the influence of fog and smoke on FSO attenuation, and [11, 12] show the change in attenuation owing to rain. In these atmospheric condition changes, the FSO link's attenuation may reach hundreds of dB/km [13], making it incapable of transmitting data without very high transmitted powers. Compared to FSO links, fiber optic transmission links require more maintenance, installation time, and expense. In the case of a link failure in typical weather conditions, the cost of maintaining the FSO link is low and negligible. Fiber optic connection requires about five times more money than FSO.

In fiber-optic communication, the transmission speed is also slower than in FSO, where the communication channel is air rather than glass [14]. Several research works have been carried out on fiber optic link-based, reliable, energy-efficient communication networks [14-17]. Previously, a few cascaded optical fibers and FSO designs have been presented [15]. FSO system atmospheric turbulence channels gamma-gamma and log-normal have been analyzed theoretically with rectangular quadrature amplitude modulation (QAM) and avalanche photodiode (APD). In weak-to-moderate turbulence, a hybrid link combines single-mode fiber with 500m free-space optics [18]. Chromatic dispersion and atmospheric turbulence were compensated using adaptive electronic equalization in a hybrid optical link.

The performance of FSO connections in severe air conditions was investigated through Mary-QAM methods. Their findings showed that as the value of M was increased, data speeds improved significantly at the expense of bit error rate performance. As a result, a trade-off between acceptable system error performance and the needed data rate must be maintained [19]. Bit Error Rate (BER) was reported over different modulation techniques over the FSO link. Gamma-gamma turbulence model was analyzed with binary phase-shift keying (BPSK), differential phase-shift keying (DPSK), and M-ary QAM modulation schemes [20]. This work showed that the BPSK scheme performed better than the other two schemes in terms of BER, and decreased connection quality was observed, especially on the M-QAM level and the linkage spectrum. However, in the hybrid fiber optic and FSO system, because both FSO and fiber optic connections are connected in a cascade between the service provider and the end-user, the critical issues of both technologies remain unresolved.

We explored the integration of fiber optics with FSO links in this work. We created a hybrid FO-FSO optic architecture that delivers data across 100 km through fiber and 0.4-1.5 km via FSO channel using QAM/PSK modulated signal. When the FSO connection is examined for different weather conditions, including rain, fog, and haze, the FSO transmission loss becomes considerable, necessitating relatively high power transmission. Simulated results are discussed in the results and discussion section.

2.0 SYSTEM DESIGN

The block diagram of the FO-FSO system is shown in Figure 2. To show the modulated data transfer and for ease of understanding, simulation purpose, fiber optic channel is considered with a fixed 100km distance, and FSO channel is varied from 0.4km to 1.5km based on its better outcome at the receiver. Parameters used in this FO-FSO system are shown in Table 1.

Table 1 Various parameters used in FO-FSO QAM/PSK system

No.	System Parameters	Values
1	Fiber optic (FO) channel	Single mode fiber
2	Dispersion	16.75 ps/nm/km
3	Attenuation	0.2dB/km
4	Fiber optic channel length	100 km
5	FSO Channel model	Gamma-Gamma Turbulence model
6	FSO length	0.4km - 1.5km
7	Weather conditions	Clear air, Haze, Fog (Moderate)
8	Optical amplifier	10dB and 20dB gain

Data is communicated over free space through light propagation through a transmission to a receiving telescope in a free-space optical communication system that does not necessitate an optical fiber line. Figure 1 depicts the fundamental block diagram of the FSO system, where the laser source is used to generate the carrier signal, the optical modulator to impose information data into light, and the electrical modulator is used on the transmitter side. In contrast, filters, amplifiers, and demodulators are used on the receiver side. A point-to-point atmospheric channel is used to carry data wirelessly. The faster data rate, more secure (line of sight-LOS), less power and mass than RF communication systems, and more flexibility are all advantages of FSO communication. In the FSO system, implementing an atmospheric channel between the transmitter and receiver is a significant challenge

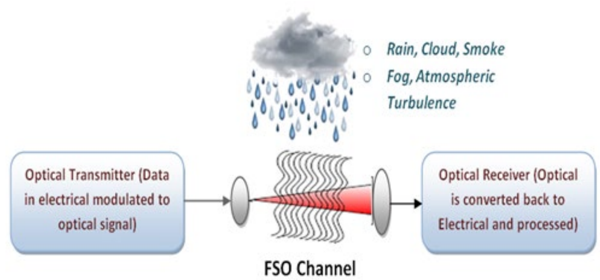

Figure 1 Free Space Optical (FSO) System Block diagram

Different weather conditions, such as rain, fog, clouds, and air turbulence, create signal attenuation. The attenuation and bit error rate are the worst when there is much fog. Because of the point-to-point communication infrastructure, misalignment of both sending and receiving antennas is also a significant problem for transmission.

2.1 FSO Channel Model

Atmospheric channel models such as the gamma-gamma turbulence model, rician fading, and rayleigh model represent the environment and its meteorological conditions. These are used to investigate the mitigation of signal loss due to variation in atmospheric conditions. For the FSO system, a gamma-gamma turbulence model is utilized in this work. The Gamma-Gamma turbulence model employs two random gamma variables that differ significantly and can represent weak to strong atmospheric turbulence. A mathematical representation of the gamma-gamma distribution model is given in the equation. Its probability distribution function is expressed as [22-24]

$$f_I(I_{mn}) = \frac{2(\alpha\beta)^{\frac{\alpha+\beta}{2}}}{\Gamma(\alpha)\Gamma(\beta)} I_{mn}^{\frac{\alpha+\beta}{2}-1} K_{\alpha-\beta}(2\sqrt{\alpha\beta I_{mn}}) \quad (1)$$

where $\Gamma(*)$ - *Gamma function*, $K_v(*)$ is the *fifth*-order modified Bessel function [25], α, and β are both calculated using the following formulas based on weather conditions. [26, 27],

$$\alpha = \left[\exp\left(\frac{0.49\chi^2}{\left(1+0.18d^2+0.56\chi^{\frac{12}{5}}\right)^{\frac{7}{6}}}\right)-1\right]^{-1}$$

$$\beta = \left[\exp\left(\frac{0.51\,\chi^2\left(1+0.69\chi^{\frac{12}{5}}\right)^{\frac{-5}{6}}}{\left(1+0.9d^2+0.62d^2\chi^{\frac{12}{5}}\right)^{\frac{7}{6}}}\right)-1\right]^{-1}$$

where $\chi^2 = 0.5C_n^2 k^{7/6} L^{11/6}$, $d = (\frac{kD^2}{4L})^{1/2}$, $k = 2\pi/\lambda$.

D - the aperture of the receiving lens, in terms of its diameter, L - link distance in meters. Refractive structural parameter C_n^2 is an altitude-dependent index that ranges from $10^{-13}m^{-2/3}$ to $10^{-17}m^{-2/3}$

3.0 PROPOSED MODEL

The block diagram of the proposed QAM/PSK FO-FSO system is shown in Figure 2. Optisystem 18.0 software has been used to build and analyze this system: the transmitter, fiber optic channel, FSO channel, and receiver form up the network. The transmitter consists of a quadrature amplitude modulator and phase shift keying modulator, continuous wave (CW) laser, optical modulator – LiNb - Mach Zehnder Modulator (LiNb-MZM), and pseudo-random bit sequence (PRBS) generates information data. QAM/PSK digital modulations are performed on the electrical signal with the help of a sequence generator, which develops in-phase (I) and quadrature (Q) signals, M-ary pulse generator, and quadrature modulator. CW laser light emission has been set to 1552nm wavelength and power value sweep from -10dBm to 10dBm. The electrically modulated signal is applied to LiNb-MZM, which converts electrical to an optical signal to transmit over the channel. MZM modulator changes the intensity of CW laser light based on electrical signal variations.

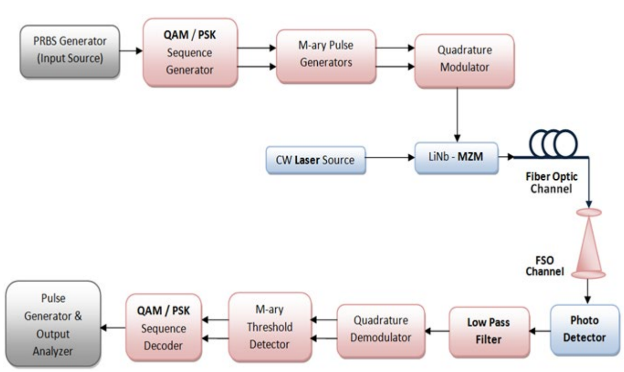

Figure 2 Fiber Optic (FO) - FSO block diagram

For this analysis, the fiber optic channel is set to 100km, and fiber attenuation has been considered the expected value of 0.2dB/km. No compensation techniques are considered for fiber channels since the analysis is for various atmospheric conditions of the FSO channel connected next to the fiber link. Optical amplifiers are used before and after the FSO channel with 10dB and 20dB gain, respectively. A PIN photodetector converts the incoming optical signal to electrical signals. An electrical amplifier with a gain of 34dB improves the strength of the incoming signal, and the Gaussian bandpass filter passes only the required frequency to the QAM/PSK demodulator. The demodulator produces the desired data in the electrical domain. An electrical constellation visualizer displays the mapped symbols received with noise. The whole network is modeled to transfer the data in an optical communication system to reach a last-mile connection.

3.1 Simulation Model And Atmospheric Attenuation Calculation

The Beer-Lambert Law explains how laser power is affected by the atmosphere. [28]:

$$\tau = e^{-\sigma R} \quad (2)$$

$\tau = Transmittance$, $\sigma = Attenuation\ coefficient$

σ is 0.1 (0.43dB/km) for visibility upto 23 km; 1 (4.3dB/km) for visibility upto 4 km, 10 (43dB/km) for visibility upto 0.5 km.

A scattering or attenuation coefficient can be calculated using [22],

$$\sigma = \frac{3.91}{V}(\frac{\lambda}{550nm})^{-q(v)} \quad (3)$$

$\sigma = atmospheric\ attenuation\ coefficient,$
$V = visibility\ (in\ km)$
$\lambda = wavelength\ (in\ nm),$
$q(v) = the\ size\ distribution\ of\ the\ scattering\ particles.$

Visibility (V in km) has been studied by Koschmieder law, a visibility model, cited in Middleton (1947) and Duntley (1948a) [29]:

$$V = \frac{3.912}{\gamma_{550nm}} \quad (4)$$

Also, the attenuation prediction formula has been studied [30, 31]

$$\gamma(\lambda) = \frac{17}{V}\left(\frac{\lambda}{550}\right)^{-q(v)} \quad (5)$$

In the above Equation, *q(v)* is the particle size distribution coefficient in (5). The atmospheric signal attenuation can be expressed with the help of some models, and to calculate the FSO link budget, the Kruse model is commonly used.

$$q(v) = \begin{cases} 1.6 & if\ \ V > 50km \\ 1.3 & if\ \ 6km < V < 50km \\ 0.585V^{1/3} & if\ \ V < 6km \end{cases}$$

In dense fog, the particle size distribution coefficient q was estimated using the above model for the visibility less than 6km is $0.585V^{1/3}$ and the value of visibility, *V*<1km, was proposed by the Kim model as,

$$q(v) = \begin{cases} 1.6 & if\ V > 50km \\ 1.3 & if\ 6km < V < 50km \\ 0.16V + 0.34 & if\ 1km < V < 6km \\ V - 0.5 & if\ 0.5km < V < 1km \\ 0 & if\ V < 0.5km \end{cases}$$

For tropical regions where fog attenuation is not taken into account and only haze attenuation is measured, the Kruse model is acceptable because we are not required to consider the visibility of less than 1kilometer.

Table 2 Atmospheric Loss parameters in FSO system

Weather	Visibility in atmosphere (km)	dB/km, 1550nm
FOG	0.2	60
	0.5	21
HAZE	2	4
	4	2
CLEAR AIR	10	0.4
	23	0.2

For 1550 nm, the air losses (dB/km) calculated using Equation (5) are shown in Table 2. The laser wavelength in this design is 1550 nm, which is a continuous wave laser. The attenuation is computed as follows:

$$\gamma(\lambda) = \frac{17}{2}\left(\frac{1550}{550}\right)^{-(0.585*2\wedge(1/3))} = 3.95\ dB/km.$$

Attenuation of 4 dB/km is considered for haze weather conditions for the visibility of 2km. Similarly, attenuation under thin fog is calculated as approximately equal to 9 dB/km. The Attenuation calculated under thick fog is approximately equal to 16 dB/km, equal to 22 dB/km under heavy fog.

4.0 RESULT AND OBSERVATION

A powerful tool for developing and analyzing optical networks, Optisystem version 18 was used to investigate the proposed link.

4.1 Constellation Diagram Comparison

Different modulation techniques modulate the information signal, such as 4 – QAM, 8 – PSK, 16 – PSK, 16 – QAM, and 64 – QAM. Figures 3a, 3b, and 3c illustrate the constellation diagrams observed at the receiver for all modulation schemes for various ranges of FSO channels.

All the constellation diagrams shown here represent the best possible outcome of each modulation approach at the FSO link's maximum range. Signal attenuation under atmospheric conditions is considered to analyze signal dispersion, such as clear weather, haze, and fog (moderate). Their attenuations are 0.2dB/km, 4dB/km, and 21dB/km, respectively. The 4-QAM technique has improved constellation up to 1.5km of FSO channel in clear air, 1km in a haze, and signal dispersion increases as the link range increases from 1.5km.

4-QAM 8-PSK 16-PSK 16-QAM 64-QAM

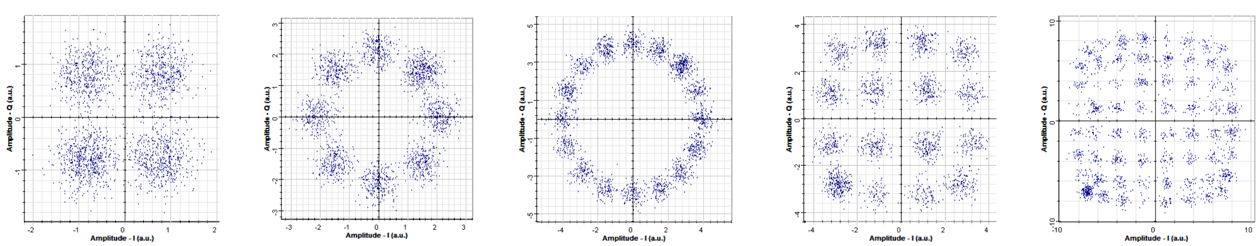

Distance 1.5km Distance 1.1km Distance 0.8km Distance 0.8km Distance 0.5km

Figure 3a Clear weather (Visibility – 23 km and Attenuation - 0.2dB/km)

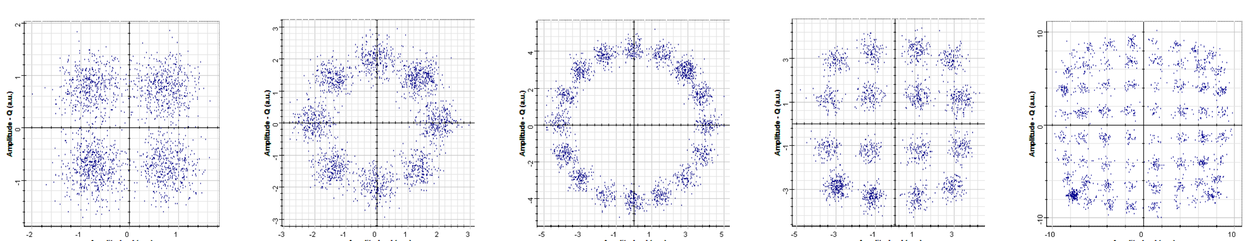

Distance 1km Distance 0.8km Distance 0.6km Distance 0.6km Distance 0.4km

Figure 3b Haze weather (Visibility – 2 km and Attenuation - 4dB/km)

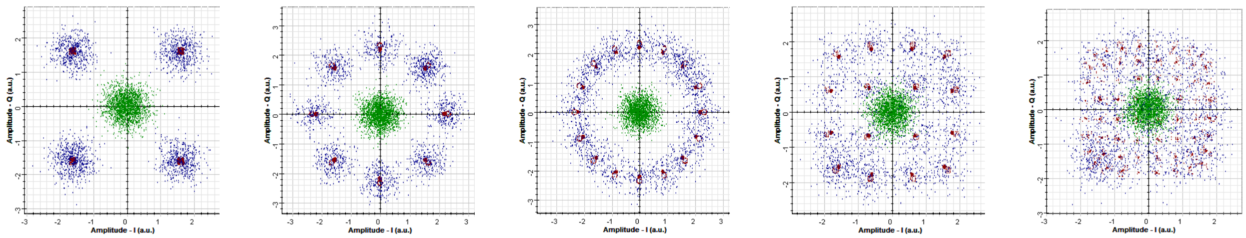

Distance 0.4km Distance 0.4km Distance 0.4km Distance 0.4km Distance 0.4km

Figure 3c Fog(Moderate) weather (Visibility – 0.5 km and Attenuation - 21dB/km)

Figure 3 Constellation diagram comparison of digital modulation technique

Signal dispersion occurs when the FSO range is increased beyond the indicated values. For clear air and haze conditions, 8-PSK has a better constellation up to 1.1km and 0.8km. The 16-PSK scheme has a better constellation of 0.8km and 0.6km. 16-QAM is better than the PSK technique for the same FSO range, i.e., 0.8km and 0.6km for 0.2dB/km and 4dB/km. 64-QAM has a limited FSO range performance because increasing the symbol mapping leads to signal identification problems. This scheme has a better constellation at 0.5km and 0.4km for clear air and haze conditions.

The FSO channel range of 0.4km is used for fog in moderate conditions to compare all modulation schemes' performance because 4-QAM maintains its higher performance. Figure 3c depicts constellations for an FO-FSO system with a 0.4km FSO channel for 21dB/km signal attenuation. Comparatively, the 4-QAM scheme produces a better result in all conditions. Also, for the same FSO channel range, the QAM technique produces a far better constellation than PSK.

4.2 EVM vs. Received Power Analysis

In a digital modulated system, the error vector magnitude (EVM) vs. bit error rate (BER) is used to evaluate the performance of the received signal. EVM may be measured using the optimized constellation diagram, and the BER parameter can calculate the error probability [21]. In this proposed system, 4-QAM techniques produce a better result for BER than other modulations.

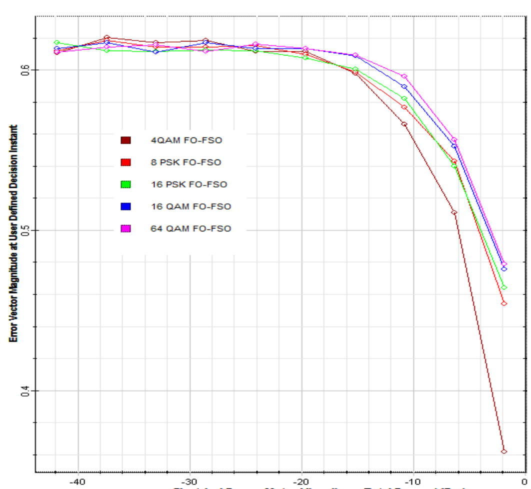

Figure 4 EVM vs. Received Power for FSO channel with 1.5km length and 0.2dB/km attenuation

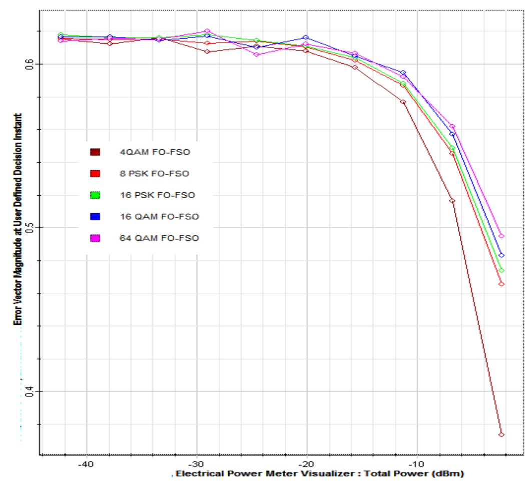

Figure 5 EVM vs. Received Power for FSO channel with 1km length and 4dB/km attenuation

We employed error vector magnitude curves and a received power at the output of a PIN photodiode in this investigation to verify the performance of the FO-FSO system. Figures 4-6 represent EVM in received power for modulation schemes 4-QAM, 8-PSK, 16-QAM, 16-PSK, and 64-QAM. In a CW laser, the input power is set as a sweep variable ranging from -10dB to 10dB. The received signals in graphs are given without forward-error correction (FEC) for the FO-FSO system. The fiber channel is 100 kilometers long, while the FSO channel is 0.4 to 1.5 kilometers long. Optical amplifiers are placed in the FSO channel's front and back ends.

The EVM vs. Received Power of the system is shown in Figure 4. The fiber link distance is set, and the FSO link is fixed at 1.5km for 0.2dB/km air attenuation in clear weather. Input parameters of the FSO channel such as attenuations and distance are considered with the best modulation scheme (4-QAM) for weather conditions clear air, haze, and fog in the atmospheric channel and with its better distance of 1.5km for 0.2dB/km, 1km for 4dB/km, and 0.4km for 21dB/km.

Figures 5 and 6 depict EVM for the received power at the FSO link in case of haze and moderate fog. The system with all modulation schemes is observed as increment EVM with lower received power and variable-length FSO channel in the graphs. When the received power is less than -20dBm, EVM increases instantly, and EVM drops when the received power is higher than -20dBm. Also, comparatively 4-QAM FO-FSO systems received power with EVM better than other schemes.

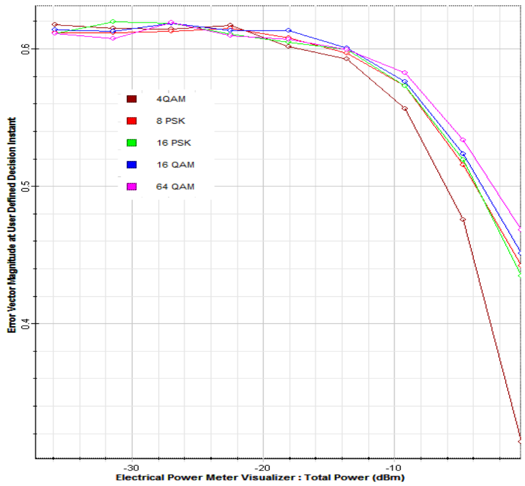

Figure 6 EVM vs. Received Power for FSO channel with 0.4km length and 21dB/km attenuation

The EVM increases for the constellation points, which become increasingly dispersed as the FSO channel length and atmospheric attenuation value increase. The proposed systems results are compared with existing works in Table 3. The comparison is made with the communication system having both fiber optic and FSO channels. At the receiver end of a real-time system, signal processing (DSP) is required. However, we did not use DSP in our simulation because the simulation settings for this system model are considered ideal. The signal dispersion may be considerably compensated by using DSP, and the length of the FO-FSO channel can be significantly extended.

Table 3 Comparison of proposed system with existing works

Reference	Technique	Channel	Attenuation	Range
Ref [18]	Adaptive electronic equalization	Fiber Optic Channel FSO Channel	0.2 dB/km 0.2 dB/km	20 km 0.5 km
Ref [15]	WDM PON Impaired by Four-Wave Mixing	Fiber Optic Channel FSO Channel	0.2 dB/km 21 dB/km	20 km Test for 2.5 km, 2.6 km
Ref [6]	long-term evolution (LTE) M-QAM signals	Fiber Optic Channel FSO Channel	0.2 dB/km 4 dB/km	5 km 2 m
Proposed System	M-PSK/M-QAM signals	Fiber Optic Channel FSO Channel	0.2 dB/km 0.2 dB/km 4 dB/km 21 dB/km	100 km 1.5 km 1 km 0.4 km

5.0 CONCLUSION

For 100 km of fiber optic channel with 0.4-1.5km of free space optic channel, the performance of the proposed FO-FSO system with QAM/PSK digital modulation schemes has been investigated. This analysis aims to identify the capacity of various digital modulations in optical connections to develop a last-mile communication system. Attenuations in channels are noticed at the receiver side in constellation diagram verification under varied weather conditions. Error vector magnitude for received power is observed for variable input power. The observation results of the proposed system show that 4-QAM produces an effective output under various weather conditions and ranges. Also, the QAM modulation scheme showed a better outcome than PSK modulation.

Acknowledgement

The Authors would like to express gratitude to the technical support provided by the Electronics and Communication Engineering Department, SRM Institute of Science and Technology, Delhi-NCR campus.

References

[1] Garg, A.K., Janyani, V., Batagelj, B., Abidin, N.Z. and Bakar, M.A., 2021. Hybrid FSO/fiber optic link based reliable & energy efficient WDM optical network architecture. *Optical Fiber Technology*, 61: 102422. DOI: https://doi.org/10.1016/j.yofte.2020.102422

[2] Badar, N. and Jha, R.K., 2017. Performance comparison of various modulation schemes over free space optical (FSO) link employing Gamma–Gamma fading model. *Optical and Quantum Electronics,* 49: 1-10. DOI: https://doi.org/10.1007/s11082-017-1025-4

[3] Alkholidi, A.G. and Altowij, K.S., 2014. Free space optical communications—theory and practices. *Contemporary Issues in Wireless Communications*, 159-212. DOI: https://doi.org/10.5772/58884

[4] Trung, H.D., Ai, D.H. and Pham, A.T., 2015. Average channel capacity of free-space optical MIMO systems over atmospheric turbulence channels. *ASEAN Engineering Journal*, 5(2): 57-66. DOI: https://doi.org/10.11113/aej.v5.15462.

[5] Jia, Z., Yu, J., Chowdhury, A., Ellinas, G. and Chang, G.K., 2007. Simultaneous generation of independent wired and wireless services using a single modulator in millimeter-wave-band radio-over-fiber systems. *IEEE Photonics Technology Letters*, 19(20): 1691-1693. DOI: https://doi.org/10.1109/LPT.2007.905196

[6] Nguyen, D.N., Bohata, J., Komanec, M., Zvanovec, S., Ortega, B. and Ghassemlooy, Z., 2019, November. Optical Hybrid Fiber/Free-Space and 25 GHz Wireless Transmission using LTE M-QAM Signals. In *2019 22nd International Symposium on Wireless Personal Multimedia*

Communications (WPMC) 1-6. IEEE. DOI: https://doi.org/10.1109/WPMC48795.2019.9096169

[7] Trung, H.D., Ai, D.H. and Pham, A.T., 2015. Average channel capacity of free-space optical MIMO systems over atmospheric turbulence channels. *ASEAN Engineering Journal*, *5*(2): 57-66. DOI: https://doi.org/10.11113/aej.v5.15462

[8] Kumar, M.V. and Kumar, V., 2022. Mitigation of Atmospheric Attenuations in Hybrid Fiber-optical and Free-space Optical Channel for Last-mile Communication System. *IEIE Transactions on Smart Processing & Computing*. *11*(1): 64-72. DOI: https://doi.org/IEIESPC.2021.11.1.64

[9] Zhang, R., Ma, J., Wang, Z., Zhang, J., Li, Y., Zheng, G., Liu, W., Yu, J., Zhang, Q., Wang, Q. and Liu, R., 2014. Full-duplex fiber-wireless link with 40 Gbit/s 16-QAM signals for alternative wired and wireless accesses based on homodyne/heterodyne coherent detection. *Optical Fiber Technology,* 20(3): 261-267. DOI: https://doi.org/10.1016/j.yofte.2014.02.008

[10] Ijaz, M., Ghassemlooy, Z., Pesek, J., Fiser, O., Le Minh, H. and Bentley, E., 2013. Modeling of fog and smoke attenuation in free space optical communications link under controlled laboratory conditions. Journal of Lightwave Technology, 31(11): 1720-1726. DOI: https://doi.org/10.1109/JLT.2013.2257683

[11] Zabidi, S.A., Islam, M.R., Al Khateeb, W. and Naji, A.W., 2011, May. Investigating of rain attenuation impact on free space optics propagation in tropical region. In 2011 4th International Conference on Mechatronics (ICOM) 1-6. IEEE. DOI: https://doi.org/10.1109/ICOM.2011.5937121. (2011).

[12] Al-Gailani, S.A., Mohammad, A.B. and Shaddad, R.Q., 2013. Enhancement of free space optical link in heavy rain attenuation using multiple beam concept. *Optik*, 124(21): 4798-4801. DOI: https://doi.org/10.1016/j.ijleo.2013.01.098.

[13] Malik, A. and Singh, P., 2015. Free space optics: current applications and future challenges. *International Journal of Optics*, 2015: 1-7. DOI: https://doi.org/10.1155/2015/945483.

[14] Willebrand, H.A. and Ghuman, B.S., 2001. Fiber optics without fiber. IEEE spectrum, 38(8): 40-45. DOI: https://doi.org/10.1109/6.938713.

[15] Pham, T.V., Nguyen, T.V., Nguyen, N.T., Pham, T.A., Pham, H.T. and Dang, N.T., 2020. Performance analysis of hybrid fiber/FSO backhaul downlink over WDM-PON impaired by four-wave mixing. *Journal of Optical Communications,* 41(1): 91-98. DOI: https://doi.org/10.1515/joc-2017-0127.

[16] [16] Garg, A.K., Madavi, A.A. and Janyani, V., 2017. Energy efficient flexible hybrid wavelength division multiplexing-time division multiplexing passive optical network with pay as you grow deployment. Optical Engineering, 56(2): 026119-026119. DOI: https://doi.org/10.1117/1.OE.56.2.026119.

[17] Garg, A.K., Janyani, V. and Batagelj, B., 2020. Ring based latency-aware and energy-efficient Hybrid WDM TDM-PON with ODN interconnection capability for smart cities. *Optical Fiber Technology,* 58: 102242. DOI: https://doi.org/10.1016/j. yofte.2020.102242.

[18] Nguyen, D.N., Zvanovec, S. and Ghassemlooy, Z., 2019. Mitigation of dispersion and turbulence in a hybrid optical fibre and free-space optics link using electronic equalisation. *Optik,* 196: 163154. DOI: https://doi.org/10.1016/j.ijleo.2019.163154

[19] Vinoth Kumar Mani, Vinod Kumar, 2022. Free-space optical channel performance under atmospheric losses using orthogonal frequency division multiplexing. *Indonesian Journal of Electrical Engineering and Computer Science*, 25(3): 1571~1579. DOI: http://doi.org/10.11591/ijeecs.v25.i3.pp1571-1579

[20] Singh, H. and Arora, M., 2015. Comparison of bit error rate performance of different modulation techniques over turbulent FSO link. International Journal of Computer Applications, 109(12): 20-24. DOI: http://doi.org/10.5120/19241-0973

[21] Fatadin, I., 2016, April. Estimation of BER from error vector magnitude for optical coherent systems. In *Photonics* 3(2): 21. Multidisciplinary Digital Publishing Institute. DOI: https://doi.org/10.3390/photonics3020021

[22] Kim, I.I., McArthur, B. and Korevaar, E.J., 2001, February. Comparison of laser beam propagation at 785 nm and 1550 nm in fog and haze for optical wireless communications. In *Optical wireless communications III* 4214: 26-37). Spie. DOI: https://doi.org/10.1117/12.417512

[23] Al-Habash, M.A., Andrews, L.C. and Phillips, R.L., 2001. Mathematical model for the irradiance probability density function of a laser beam propagating through turbulent media. *Optical Engineering,* 40(8): 1554-1562. DOI : https://doi.org/10.1117/1.1386641

[24] Andrews, L.C., Phillips, R.L. and Hopen, C.Y., 2001. *Laser Beam Scintillation With Applications* 99. SPIE press. DOI: https://doi.org/10.1117/3.412858

[25] Bayaki, E., Schober, R. and Mallik, R.K., 2008, November. Performance analysis of free-space optical systems in gamma-gamma fading. In IEEE GLOBECOM 2008-2008 IEEE Global Telecommunications Conference 1-6. IEEE. DOI: https://doi.org/10.1109/GLOCOM.2008.ECP.548.

[26] Sharma, O.P., Janyani, V. and Sancheti, S., 2007, December. Analysis of raised cosine filtering in communication systems. In 2007 Third International Conference on Wireless Communication and Sensor Networks 9-12. IEEE. DOI: https://doi.org/10.1109/WCSN.2007.4475737

[27] García-Zambrana, A., Castillo-Vázquez, C. and Castillo-Vázquez, B., 2010. On the capacity of FSO links over Gamma-Gamma atmospheric turbulence channels using OOK signaling. *EURASIP Journal on Wireless Communications and Networking,* 2010: 1-9. DOI: https://doi.org/10.1155/2010/127657.

[28] Al-Habash, M.A., Andrews, L.C. and Phillips, R.L., 2001. Mathematical model for the irradiance probability density function of a laser beam propagating through turbulent media. *Optical engineering,* 40(8): 1554-1562. DOI: https://doi.org/10.1117/1.1386641

[29] Byers, H.R., Landsberg, H.E., Wexler, H., Haurwitz, B., Spilhaus, A.F., Willett, H.C., Houghton, H.G. and Middleton, W.K., 1951. Visibility in Meteorology. *Compendium of Meteorology: Prepared under the Direction of the Committee on the Compendium of Meteorology*, 91-97. DOI: https://doi.org/10.1007/978-1-940033-70-9_7

[30] Srivastava, D., Kaur, G., Singh, G. and Singh, P., 2020. Evaluation of atmospheric detrimental effects on free space optical communication system for Delhi weather. *Journal of Optical Communications*. DOI: https://doi.org/10.1515/joc-2019-0078

[31] Kruse, P.W., McGlauchlin, L.D. and McQuistan, R.B., 1962. Elements of infrared technology: Generation, transmission and detection. New York: Wiley. DOI: https://doi.org/10.1126/science.137.3524.123.a